Available online at www.sciencedirect.com
SCIENCE DIRECT
NDT&E International 39 (2006) 184–194
NDT&E international
www.elsevier.com/locate/ndteint

Novel nonlinear-modulation acoustic technique for crack detection

Vladimir Zaitsev[a,*], Veniamin Nazarov[a], Vitaly Gusev[b], Bernard Castagnede[b]

[a]*Institute of Applied Physics RAS, 46 Uljanova Street, Nizhny Novgorod 603950, Russian Federation*
[b]*Université du Maine, Avenue Olivier Messiaen, 72085 Le Mans, Cedex 09, France*

Available online 19 September 2005

Abstract

Novel nonlinear-modulation methods for crack detection are discussed. The approach is based on the so-called cross-modulation effect consisting of the modulation transfer from an intensive, initially slowly amplitude-modulated stronger (pump) excitation to the probe signal. Advantage of this technique is a very flexible choice of the operation frequencies, since their ratio for both carriers and the modulation may be rather arbitrary. This in its turn allows one to effectively use the sample resonances in order to achieve the necessary level of the pump excitation and to ameliorate conditions for detection of the modulation sidelobes for the probe wave. Unlike higher harmonic-generation methods the initial nonlinear distortions of the pump and probe excitations (e.g. due to nonlinearities in the electronics) are not critical for this technique. In the paper we summarise results of recent test experiments that indicated high sensitivity of the new technique.

Keywords: Crack detection; Nonlinear acoustics; Wave modulation

1. Introduction

Exploitation of nonlinear vibro-acoustic effects for diagnostics and, in particular, for early crack detection is an emerging technique, which is rapidly progressing during last several years after pioneering encouraging results (e.g. [1–6]). Among other nonlinear effects such as, for example, observation of higher harmonics generation in the damaged sample, the use vibro-acoustical interactions of a modulation type yields several advantages (see e.g. [7–11]). In the conventional variants [7–11] of this technique the increased modulation depth for a weaker probe wave under the action of another intensive low-frequency wave or vibration (often called 'pump') is used as a sign of damage appearance.

A modulation approach was used in the very first (to our knowledge) patented nonlinear method of crack detection [2], whose principle was clearly described in the following formulation: 'Size of Crack the material specimen or structure having a crack to be detected is subjected to tensile or compressive forces due to excitation caused by low frequency sound waves or mechanical vibrations from a generator, thus changing the effective size of the crack in the specimen. An ultrasonic search unit is used to follow modulations of reflected energy at the crack interface due to variation of the effective size of the crack'. Initially this method was realized using analog hardware [2], and recently the activity in developing of this approach has been intensified again benefiting possibilities of modern digital signal processing [12–16].

This method is very close to the conventional linear pulse-echo technique supplemented with an additional, lower-frequency pump source in order to produce the crack modulation. The latter provides the possibility to discriminate echo-signals produced by highly compliant cracks between signals from other scatters (boundaries, near spherical or cylindrical technological holes, etc.), whose reflection strength is not influenced by the pump excitation. It is essential that the principle of this method implies that the defects should be strong enough obstacles for the propagating waves in order to produce noticeable reflection (scattering). The additional pump action serves only for better discrimination between the crack echo-signal and signals produced by other inhomogeneities and boundaries.

After the pulse-echo modulation approach [2], more recently [7] it was also demonstrated that even a rather weak damage may also induce strong modulation of a probe excitation under the action of an additional low-frequency pump, although the scattering strength of the defect is very small, since its size is much smaller than the length of

* Corresponding author.. Tel.: +7 8312 16 4872; fax: +7 8312 36 5976.
E-mail address: vyuzai@hydro.appl.sci-nnov.ru (V. Zaitsev).

0963-8695/$ - see front matter © 2005 Elsevier Ltd. All rights reserved.
doi:10.1016/j.ndteint.2005.07.007

the sounding probe wave (see additional examples in [8–11]). In particular, both the probe and pump waves could be continuous and excited at eigenfrequencies of the sample. In the latter case, the defects are often so small in the scale of the elastic wave length that the reflection from the defects cannot be singled out at all in contrast to the aforementioned pulse-echo approach [2,12–16]. However, for detection of even such a small crack-like damage in a sample this modulation technique has proven to be very sensitive. The defect localization even for (quasi-) continuous excitations can be also possible using additional analysis of differences in the modulation response for different spatial distributions of the pump and probe waves. As a disadvantage of this method it may be noted that the necessity to produce an intensive low-frequency pump action often causes complication of feasibility of the technique. For example, essentially different types of actuators may be required (for example, a piezo-source for the higher-frequency probe wave and a powerful vibration bench for the low-frequency pump). Another disadvantage is connected to the fact that normally it is convenient to excite both the pump and the probe waves tuning them to eigenmodes of the sample. However, the combination frequencies of the modulation components may appear at rather arbitrary positions with respect to the sample resonance peaks. This fact complicates the observation of the modulation sidelobes and estimation of the modulation depth, whose apparent magnitude is strongly affected by the sample resonance structure.

Recently, a new variant [17,18] of the nonlinear-modulation technique was successfully tested for detecting a weak damage. The new method is based on the so-called cross-modulation effect consisting in the transfer of modulation from an intensive, initially slowly amplitude-modulated pump excitation to the probe signal. The carrier frequency of the latter may be either lower or comparable, or higher than that of the pump signal. In order to underscore the difference and similarity with the conventional modulation technique (that is with high-by-low frequency wave modulation) the cross-modulation principle is schematically shown in Fig. 1.

It is interesting that the nonlinear cross-modulation effect first was discovered for radiowaves interacting in the inonosphere over 70 years ago. It was named the Luxemburg–Gorky (LG) effect after the location of the radio-stations, whose powerful radiation caused the modulation transfer to carrier waves emitted by other stations. Until recently, however, the analogs of this effect for elastic waves have not been discussed [17,18]. As it has been verified, this variant of the modulation technique keeps all positive features of the conventional modulation scheme earlier tested in nonlinear acoustics. An additional advantage of this technique is the very flexible, independent choice of both carrier frequencies as well as the modulation frequency. This in its turn makes possible to effectively use the sample resonances in order to achieve the necessary level of the pump excitation and to ameliorate conditions for detection of the modulation sidelobes. In particular, the modulation frequency may be readily chosen low enough in order to place the sidelobes within the same resonance peak to which the probe wave is tuned. This provides favourable conditions for detection of the modulation sidelobes around the probe wave carrier frequency and eliminates strong distortion of the apparent modulation depth. Besides, since the pump and probe carrier frequencies should not be strongly separated in this scheme, similar (e.g. piezoceramic) types of the actuators may be effectively used for the both waves. Unlike harmonic-generation methods the initial nonlinear distortions of the pump and probe excitations (e.g. higher harmonics in the sounding waves' spectra due to nonlinearities in the electronics) are not critical for this technique. Test experiments with samples containing small cracks indicated very high sensitivity of the new technique.

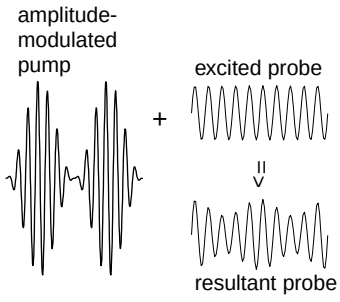

Fig. 1. Schematically shown cross-modulation of a probe wave caused by an amplitude-modulated pump excitation.

2. Why structure-sensitivity of nonlinear effects is so high?

Many publications related to the observation of nonlinear effects in damaged solids report that 'structure-sensitivity' of nonlinear properties (that is magnitude of their variations induced by a damage in the sample) is often much higher than the complementary variations in the linear elastic parameters(see e.g. [19,20])). However, the origin of such a high contrast between variations in linear versus nonlinear properties in many cases seems to be understood not clearly enough. This situation has an essential physical reason: nonlinearity manifestations are much more diverse compared to the linear ones and, besides, apparently very similar nonlinear effects may be caused by essentially different nonlinear physical mechanisms.

Quite often nonlinearity is considered in terms of the nonlinear elasticity only (see e.g. [11]), whereas actually in real cases similar effects may be caused either by nonlinear elasticity or, for example, amplitude-dependent dissipation with essentially different physics, which may be either of a nonhysteretic [9] or a hysteretic [19] type. The hysteretic nonlinearity, in its turn, comprises both the nonlinear elasticity and the nonlinear dissipation. Ample

understanding of the actual underlying mechanisms is necessary for optimization of practical implementation of the nonlinear methods. Here, we briefly elucidate the reasons of high 'structural sensitivity' of the nonlinear properties of damaged samples containing high-compliant crack-like defects.

2.1. Crack-induced elastic nonlinearity

We start with the case of purely elastic nonlinearity. It is well known that real cracks are normally not simple planar cuts inside the intact material, but contain inner contacts. The contribution of the contacts to the elastic stress is often described by the Hertzian nonlinearity [21], which in the simplest case yields the following stress–strain relationship at the contacts:

$$\sigma(\varepsilon) = B\varepsilon^{3/2}H(\varepsilon), \tag{1}$$

where factor B depends on elastic moduli of the individual asperities and their sizes, and the Heaviside function $H(\varepsilon)$ indicates that only compressed contacts (here we assume sign σ, $\varepsilon > 0$ for the compression) contribute to the stress in the material. Functional relationship (1) is quite universal and can be applied not only to circular contacts (between two spherical asperities or a sphere and a plane), but to elongated contacts between bodies whose shape near the contact can be approximated by second-order surfaces. These geometrical features are accounted by factor B in Eq. (1). The initial contact preloading can be characterized by some static contact pre-strain. We denote the mean value of this static strain ε_0. In the case of contacting spheres of radius R it is defined as $\varepsilon_0 = \Delta_0/R$, where Δ_0 is the mutual approach of the spheres' centres. In the case of contacts between crack's lips value ε_0 defined above is much greater that the mean strain in the bulk of the surrounding intact material, and only for granular materials contact pre-strain roughly corresponds to the visible macroscopic strain (although value $\varepsilon_0 = \Delta_0/R$ typically is much greater than the strain in the bulk of the grains). This static pre-strain ε_0 determines the linear elastic modulus $d\sigma(\varepsilon_0)/d\varepsilon$ of each contact subjected to oscillating perturbations, whose strain $\tilde{\varepsilon}$ and stress $\tilde{\sigma}$ are significantly smaller than the static values, $\tilde{\varepsilon} \ll \varepsilon_0$, $\tilde{\sigma} \ll \sigma_0 = \sigma(\varepsilon_0)$. In real materials, however, the initial loading of the contacts may be essentially unequal, so that along with contacts bearing some average loading there are essentially weaker loaded contacts, which also give their contributions to the resultant stress in the material. Singling out explicitly the static and the oscillating parts in stress and strain, the contributions of the average loaded and an initially unloaded contact to the stress in the material may be rewritten as:

$$\sigma_0 + \tilde{\sigma} = B(\varepsilon_0 + \tilde{\varepsilon})^{3/2}H(\varepsilon_0 + \tilde{\varepsilon}) + B(\mu\varepsilon_0 + \tilde{\varepsilon})^{3/2}H(\mu\varepsilon_0 + \tilde{\varepsilon}). \tag{2}$$

Here $\mu\varepsilon_0$ is the initial strain for the weak contact, and coefficient $[\mu] \ll 1$ characterizes the extent of the unloading. We may allow for $\mu < 0$ in order to describe the contacts with initial gaps at the interfaces, so that they may be activated at wave strains $|\tilde{\varepsilon}| > |\mu|\varepsilon_0$. It should be specially pointed out that the static pre-strain of neighbouring contacts may differ very strongly (due to random difference between initial heights of the asperities at crack's interface), whereas the dynamic strain $\tilde{\varepsilon}$ for these contacts is practically the same and is determined by approaching of the crack lips, which produces roughly the same displacements for different contacting asperities inside the crack. For initially weakly compressed contacts with positive unloading parameter ($0 < \mu \ll 1$) and for weak enough oscillation magnitude ($|\tilde{\varepsilon}| \ll \mu\varepsilon_0$), differentiation of Eq. (2) with respect to $\tilde{\varepsilon}$ readily yields the following expression for the contribution of these contacts to the linear elastic modulus:

$$\frac{d\tilde{\sigma}}{d\tilde{\varepsilon}}(\varepsilon_0) = (3/2)B(\varepsilon_0)^{1/2} + (3/2)B(\mu\varepsilon_0)^{1/2}. \tag{3}$$

It is evident from the comparison of the first and second terms in the right-hand side of Eq. (3) that the relative contribution of the weak contacts to the linear elasticity is essentially smaller (by a small factor of $\mu^{1/2} \ll 1$) compared to the contribution of more stiff, stronger compressed contacts. This agrees with the intuitive representation that the contribution of the loosest contacts occurred in the damaged areas of the material to the linear elasticity is indeed negligibly small. However, in contrast to the linear contributions, for the higher-order nonlinear moduli, which are characterized by higher-order derivatives of Eq. (2), the contribution of the weakest unloaded contacts strongly dominates over the nonlinear contribution related to the stronger pre-compressed contacts. This statement is illustrated by the following expressions for the second and third derivatives of $\tilde{\sigma}$ with respect to $\tilde{\varepsilon}$ corresponding to the quadratic and cubic (in the vibrational strain) nonlinear terms in the power expansion of the stress–strain relationship (2):

$$\frac{d^2\tilde{\sigma}}{d\tilde{\varepsilon}^2}(\varepsilon_0) = \frac{3}{4}B(\varepsilon_0)^{-1/2} + \frac{3}{4}B(\mu\varepsilon_0)^{-1/2} \tag{4}$$

$$\frac{d^3\tilde{\sigma}}{d\tilde{\varepsilon}^3}(\varepsilon_0) = -\frac{3}{8}B(\varepsilon_0)^{-3/2} - \frac{3}{8}B(\mu\varepsilon_0)^{-3/2} \tag{5}$$

These expressions demonstrate that, for the nonlinear moduli of the order $n \geq 2$, the contribution of the weak contacts (with $\mu \ll 1$) is greater than that of the average-loaded contact by a large factor of $\sim \mu^{(3/2)-n} \gg 1$. Thus the presence of highly compliant crack-like defects containing weakly pre-compressed contacts (whose contribution to the linear elasticity is very small) may strongly increase the sample elastic nonlinearity.

The above presented simple arguments illustrate the strongly different roles of the weakest (damaged) regions in the material concerning its linear/nonlinear elasticity: in

contrast to the almost negligible contribution to the linear elasticity, the loosest contacts may play dominant role in the increase of the magnitude of nonlinear effects determined by the higher-order nonlinear elastic moduli. Thus the magnitude of nonlinear acoustic effects is selectively sensitive to the presence of such weak (damaged) regions embedded into the intact material. In particular, the factor described by Eq. (4) corresponds to the quadratic in the strain contribution to the total stress and, consequently, to the linear-in-strain correction to the elastic modulus. This contribution is responsible for the instantaneous variations of the elastic modulus under an intensive vibrational excitation and may cause modulation of a weak probe wave by an intensive low-frequency pump (as is observed in conventional modulation schemes).

The factor described by Eq. (5) corresponds to the quadratic-in-strain nonlinear correction to the elastic modulus. Via this term, a periodic pump action induces period-averaged variations in the sample elasticity. Thus this period-averaged elastic effect may, in principle, be responsible for the appearance of the cross-modulation of a probe wave under the action of an amplitude-modulated pump excitation (of the type shown schematically in Fig. 1). The transformation of phase modulation of the signal (corresponding to the variation in the elasticity) into the amplitude modulation may be obtained by tuning the probe-wave frequency at the slope of a resonance peak of the sample.

It is important to point out that the assumption of the Hertzian type of the nonlinearity of compliant defects is not obligatory for the conclusions obtained above. Strongly superior variability of the nonlinear elastic moduli compared to the complementary variations of the linear elasticity can be also readily demonstrated using rheological models of an elastic material, in which the damage is modelled by high compliant elastic inclusions with an arbitrary weak deviation from linear Hooke's law (see e.g. [22]).

2.2. Crack-induced amplitude-dependent dissipation

The above considered arguments for the dominant role of soft inner contacts in cracks concerning the increase of the sample nonlinearity are rather instructive and support the simplest representation of the acoustic nonlinearity as the nonlinear elasticity. However, the very same cracks with contacts may cause a strong modulation-type interaction between the probe and pump waves via an essentially different mechanism. Namely, pronounced amplitude modulation of the probe signal may be produced by the pump wave via its direct influence on the probe signal dissipation. Conventionally, this dissipation is mostly attributed to friction or adhesion hysteresis at crack interfaces [23,24]. However, it is physically clear (and after appearance of atomic-force microscopes this was corroborated by direct atomic-scale experiments [25]) that, for manifestation of adhesion and friction, mutual displacement at interfaces should exceed a finite threshold value roughly equal to the interatomic distance a. In this context, for a crack with diameter L, the average compressional or shear strain ε can produce maximal lateral or normal interfacial displacement $D \sim \varepsilon L$ [26,27]. The requirement $D > a$ determines the threshold strain $\varepsilon_{\text{th}} > a/L$, below which the interfacial displacement is of sub-atomic scale. For a typical interatomic distance $a \sim 3\times10^{-10}$ m and a macroscopic crack with $L \sim 10^{-3}$ m, this yields $\varepsilon_{\text{th}} \sim 0.3\times10^{-6}$, which should be exceeded in order to activate frictional and adhesional hysteretic losses. However, even at much smaller strains, the defects can efficiently dissipate elastic energy due to locally enhanced thermoelastic coupling at cracks and especially at the inner crack contacts. These losses are thresholdless and they can be essential even for rather weak probe waves with strains $\varepsilon < 10^{-8}$. The corresponding mechanism was recently considered in [27], in which we argued additionally that, in crack-containing solid samples, quite moderate pump strains $\varepsilon \sim 10^{-6}$ to 10^{-5} may significantly affect the probe wave dissipation at the inner contacts in cracks. In this context, it is well known that cracks with ratio of the opening d to characteristic crack diameter L, may be completely closed by average strain $\varepsilon \sim d/L$, typical d/L for cracks being 10^{-3} to 10^{-4}. However, at small loosely separated regions, local separation (or inter-penetration, i.e. indentation) d_{loc} of crack interfaces is much smaller than average separation d. Such contacts are extremely stress-sensitive, since due to the described geometry they are strongly perturbed by the average strain, which can be orders of magnitude smaller (roughly $d/d_{\text{loc}} \gg 1$ times) than the typical mean strain $\varepsilon \sim d/L \sim 10^{-4}$ to 10^{-3} in the material required to close the whole crack.

For the magnitude of the dissipation it is important that inner contacts in real cracks are normally not point-like, but rather strip-like due to the quasi-2D character of crack initiation. Such a shape of contacts agree with direct electron and atomic-force microscopy images of cracks normally exhibiting wavy corrugated structure of the interfaces. Due to this geometry (and the resultant strong local concentration of stress and increased temperature gradients), the inner contacts may very efficiently dissipate elastic wave energy via the thermoelastic coupling. In order to estimate the magnitude of this dissipation we applied an approximate approach, similar to that used in [21] for estimates of thermoelastic losses in polycrystals, and additionally took into account stress-concentration at the inner contacts. Thus we derived [18] the following approximate expressions for thermoelastic losses in the low-frequency limit, in the high-frequency limit and at the relaxation maximum, when the thermal wave length coincides with the width of the contact:

$$W_{\text{LF}}^{\text{dis}} = 2\pi\omega T \frac{\alpha^2 K^2}{\kappa} l^2 \tilde{L} L^2 \varepsilon^2, \quad \omega \ll \omega_l \approx \frac{\kappa}{\rho C l^2}, \tag{6}$$

$$W_{\mathrm{HF}}^{\mathrm{dis}} = \frac{2\pi}{\omega}\kappa T\left(\frac{\alpha K}{C\rho}\right)^2 \tilde{L}(L/l)^2\varepsilon^2, \quad \omega \gg \omega_l, \tag{7}$$

$$W_{\mathrm{cont}}^{\max} = 2\pi T(\alpha^2K^2/\rho C)\tilde{L}L^2\varepsilon^2, \quad \omega \approx \omega_l, \tag{8}$$

where ω is the wave cyclic frequency, T is the temperature, α is the temperature expansion coefficient of the solid, K is the bulk elastic modulus; ρ is the density; C is the specific heat, ε is the average strain, κ is the thermal conductivity, ω_l is the relaxation frequency for contact width l, L is the characteristic crack diameter and $\tilde{L}$ is the contact length. Note that, for strip-like contacts with $\tilde{L} \sim L$, the magnitude of the maximal thermoelastic losses at narrow contacts is roughly the same as at the whole crack [18]. However, the relaxation frequencies for millimetre-scale cracks are fractions of Hz for most of metals, glasses or rocks, whereas for narrow contacts, this frequency can reach kHz and even MHz band typically used in acoustic and ultrasonic experiments. Quantitatively the estimates based on Eqs. (6)–(8) indicate that the considered thermoelastic losses at the inner contacts can be rather strong and may produce pronounced modulation of the probe wave under the action of pump excitations with quite moderate-amplitudes. The relevant experimental examples will be considered below.

3. Experimental demonstrations

3.1. Cross-modulation in glass samples with thermal cracks

In order to demonstrate high sensitivity of the cross-modulation effect to the presence of defects in a solid sample we implemented an instructive experiment in the form of interaction of two longitudinal modes in a glass rod 30 cm in length and 8 mm in diameter.

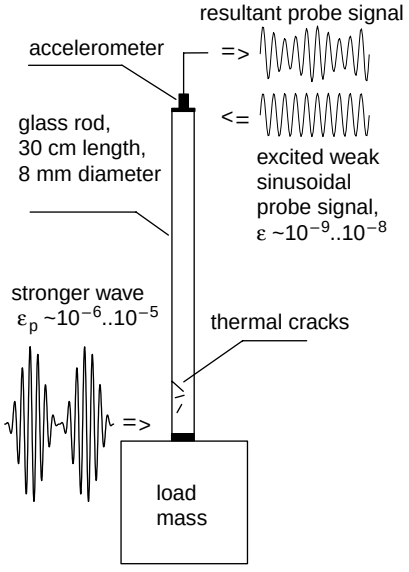

Fig. 2. Schematically shown experimental configuration.

The rod contained three corrugated thermally-produced cracks 2–3 mm in size (see the scheme in Fig. 2). The probe and pump waves were tuned to different resonance peaks of the rod (for example, to the second and first longitudinal resonances about 3.8 and 11 kHz, respectively). The modulation frequency was chosen equal to a few Hertz, so that it was convenient to observe the modulation sidelobes together with the carrier-frequency lines for the pump and the probe waves within the respective resonance peaks. Typical strain amplitudes were $\varepsilon_{\mathrm{pump}} \sim 10^{-6}$ to 10^{-5} for the pump wave and $\varepsilon_{\mathrm{prob}} \sim 10^{-9}$ to 10^{-8} for the probe wave. In reference rods without cracks, the modulation sidelobes (existing due to residual parasite nonlinearities) were 25–40 dB lower compared to the example shown in Fig. 3. In the next Fig. 4, a similar spectral record is made with a smaller resolution and in a wider band in order to simultaneously show the spectra of the probe wave and the third harmonic of the pump wave. This record clearly demonstrates that these spectra do not overlap, and thus the observed modulation cannot be attributed to the interference of the probe wave with the third harmonic of the pump. Furthermore, the carrier frequency of the pump could be chosen close to one of higher resonances of the sample (in the range 30–50 kHz), so that the pump had no spectral components in the vicinity of the probe wave frequency at all, whereas the effect of the induced cross-modulation was persistently observed.

In principle, one may suppose that the variation in the amplitude of the probe wave may be attributed, for example, to the pump-induced mismatch between the carrier frequency of the probe-wave and the sample resonance frequency, so that modulation of the pump amplitude should result in the modulation of the probe resonance position. The latter may be related to the variation of the elasticity of the nonlinearly-elastic defects (cracks) under the action of the stronger pump wave (see discussion in Section 2.1). Alternatively, the probe-wave modulation could be caused by the direct influence of the pump wave on the dissipation of

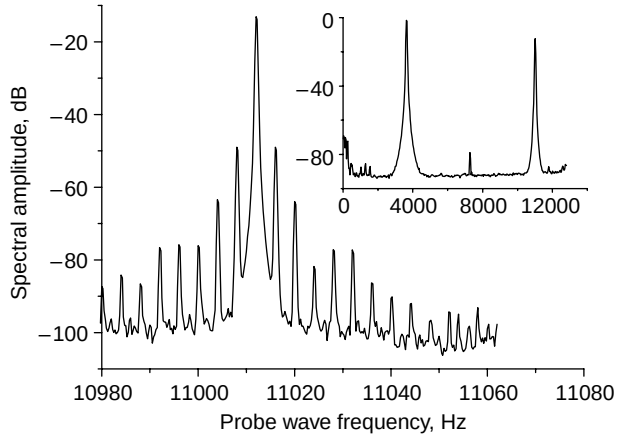

Fig. 3. Experimental spectrum of the cross modulation in the damaged glass rod. In the inset the lower-resolution spectra of the pump and probe waves are displayed.

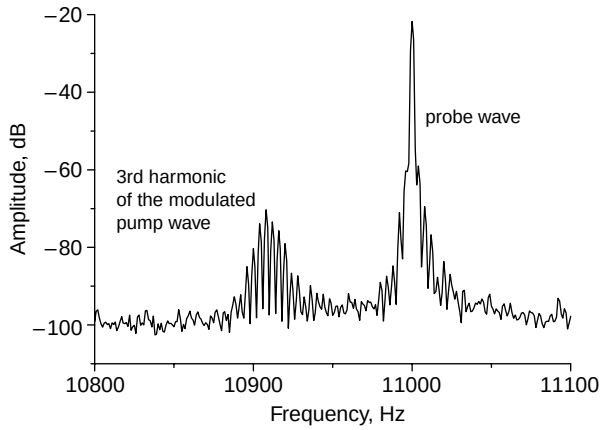

Fig. 4. Spectral record with lower resolution than in Fig. 3. The record demonstrates that the spectra of the third harmonic of the modulated pump wave (around 10,900 Hz) and the probe wave with induced cross-modulation (around 11,000 Hz) do not overlap.

the probe signal (that is on the quality factor of the probe wave resonance). Certainly, the elastic and dissipative effects could be mixed.

In order to clarify the actual mechanism we investigated the shapes of resonance curves for the probe signals at different amplitudes of the pump action. To this end instead of initially monochromatic probe waves we used probe signals in swept-sine or chirp regimes and observed variations of the whole shape of the probe-wave resonance peaks. The resonance curves presented in Fig. 5 indicate that primarily the dissipation, not the elasticity, is affected by the stronger wave in the discussed case. Indeed, the shapes of the resonance peaks obtained without the pump wave and at different pump amplitudes show clearly that the frequency of the resonance maximum for the probe wave remains constant with a high accuracy (in the scale of the resonance width), whereas the height of the resonance peak exhibits quite significant (10–12%) variations. It is essential to point out that the noticeable change of the resonance shape occurs

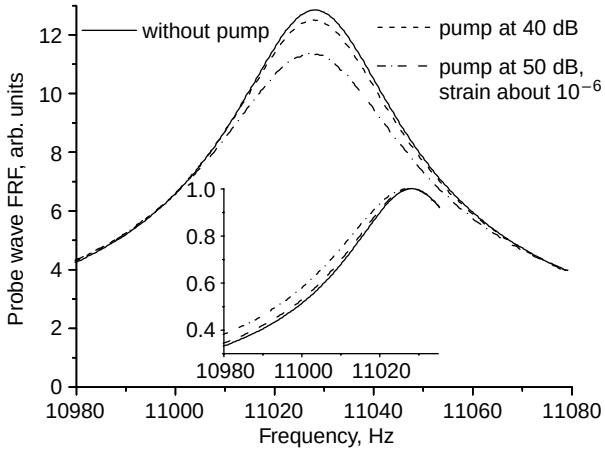

Fig. 5. Probe wave frequency-response functions obtained at different pump amplitudes. The inset displays widening of the normalized resonance curves (for clarity only the left halves are shown).

only near its maximum (within ± 20 Hz), whereas the wings of the resonance curve remain practically unperturbed. This could not be attributed to the manifestation of the overload in the preamplifier. First, the absence of the overload was carefully controlled and, second, the eventual pump-induced nonlinear saturation in the electronics should modify the amplitude of the weak probe wave uniformly (that is by the same factor at the wings and near the resonance maximum) instead of the observed selective variation of the maximum only as shown in Fig. 5. This indicates that the origin of the effect is indeed related to the nonlinearity in the material, but not to the electronics. Second, the negligibly small resonance frequency shift corroborates clearly that the pump predominantly affects the quality factor (that is dissipation) for the probe wave resonance, whereas the role of the pump-induced variations in the elasticity is negligible for the observed modulation.

Indeed, we have argued above in Section 2.2 that the weak contacts (inside in the thermal cracks) can be significantly perturbed by the pump wave with strains $\varepsilon_{\text{pump}} \sim 10^{-6}$–$10^{-5}$ used in the discussed experiments. Due to the asymmetric response of the contacts with respect to loading and unloading, the applied oscillating stress can noticeably change their period-averaged width, thus essentially affecting the dissipation of the probe wave at the contacts. Eqs. (6)–(8) allow us to estimate the magnitude of energy losses of the acoustic wave over its period, and knowing the rod size one may estimate the magnitude of the elastic energy stored in the resonator. The ratio of these values readily yields the contribution of the contacts to the decrement of the probe wave resonance (that is the parameter inverse to the quality factor). Performing such a procedure we have found that the magnitudes and frequencies, at which the amplitude-dependent variations in dissipation were observed (see, for example, Fig. 5), reasonably agree with estimates based on Eqs. (6)–(8). In these estimates we assumed existence of 1–2 elongated (of 2–4 mm in length) inner contacts between corrugated surfaces of 2–3 thermal cracks. Quantitatively, the estimates made for typical parameters of glass show that the thermoelastic dissipation at the inner contacts suffices to explain the observed 10–12% variation in the magnitude of the resonance quality factor $Q \sim 300$–350 for the probe wave (as in the examples in Fig. 5).

In these experiments, the performed comparison with reference samples without defects confirmed that the observed nonlinear phenomena indeed were related to the presence of cracks, whose number and sizes could be readily estimated visually in the transparent glass. The size and shape of the inner contacts could not be so easily evaluated, but the grating-like (not circular) character of the optical interference pattern at the corrugated crack interfaces unambiguously demonstrated their wavy shape and clearly indicated that the contacts between such interfaces should have an elongated strip-like form, as it was assumed in the estimates of the dissipation at the contacts.

3.2. Cross-modulation in glass sample with artificial crack-like defect

Another experimental demonstration of the high-sensitivity of the cross-modulation effect was obtained for a thick glass plate $230\times190\times14.5$ mm in sizes. In order to demonstrate high sensitivity of the nonlinear effects to the presence of crack-like defects in the sample and, in contrast, to prove that complex boundaries, technological holes, etc. are not important for the nonlinear interaction, we prepared the sample in a special manner. The experimental arrangement is schematically shown in Fig. 6. In order to model technological holes and cracks in the sample we made two cuts about 1 mm in thickness and 15 mm in depth in the directions perpendicular to two neighbouring plate edges. The sample prepared in such a manner served as a reference one and presence of the cuts did not influence the background weak nonlinearity of the system (which comprised both the weak atomic nonlinearity of the material and imperfectness of the electronics). Further, when a small steel plate was tightly inserted in one of the cuts, the latter imitated a crack-like defect with the apparent interface area of 2–4 mm^2 (certainly, the actual contact area of the asperities was much smaller). The sinusoidal probe wave and slowly amplitude-modulated pump wave were excited by two piezo-actuators glued to the opposite plate edges. The detailed structure of the acoustic field was not studied in this experiment, but much like in the above described resonance-bar examples the maximal attainable strain amplitudes for compressional bulk modes were between 10^{-6} and 10^{-5} corresponding to the maximal amplifier output 60 dB.

The installation of a steel insert in either of the cuts caused appearance of a rather pronounced modulation of the probe signal as shown in Fig. 7(a). The pump-wave frequency in this technique could be chosen either lower or higher than the probe-wave frequency. In particular, for the example shown in Fig. 7(a) the pump frequency was about 54 kHz that is higher than the probe-wave frequency

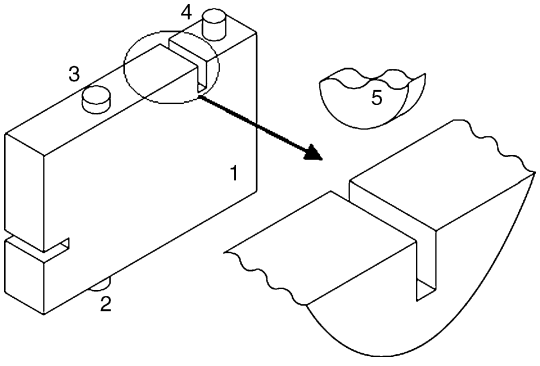

Fig. 6. Schematically shown experimental setup with artificial crack-like defect: 1—thick glass plate with two saw-cuts; 2 and 3—piezo-actuators to excite pump and probe signals; 4—accelerometer; 5—small metal disc that could be tightly inserted into the cuts.

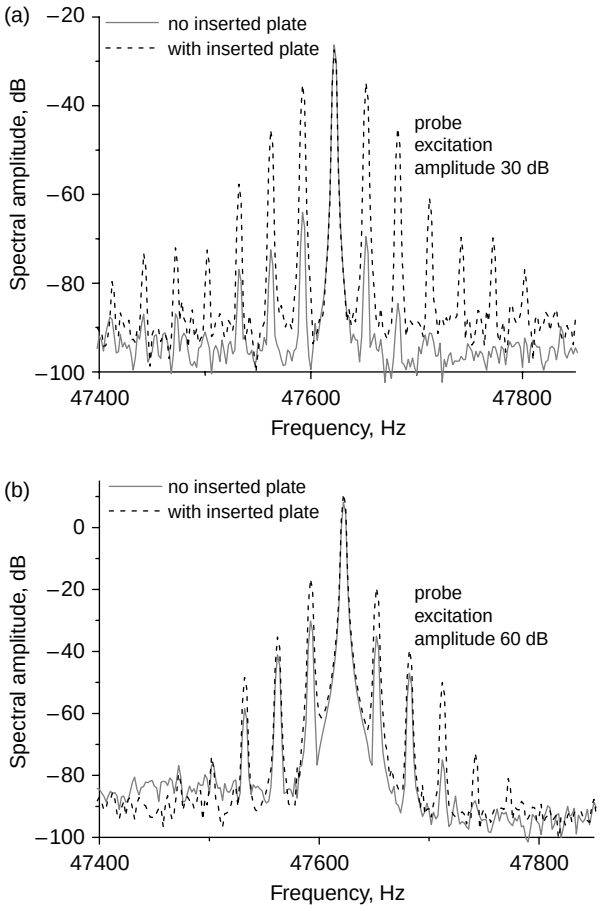

Fig. 7. Examples of the probe wave modulation spectra for the sample without the insert in the cut (no crack) and with the insert (artificial crack-like defect).

about 47.6 kHz. For plots in Fig. 7(a) the magnitude of the sample excitation corresponded to 60 dB for the pump and 30 dB for the probe wave.

It is essential to point out an important experimentally observed feature of the cross-modulation, which also agrees well with the above presented arguments about the perturbation of the state of contacts at crack's interfaces. Namely, it could be expected that, at high enough amplitudes, the probe wave itself would be able to significantly perturb the state of the contacts, so that the additional pump-action should not produce as strong influence as in the case of weaker probe-wave amplitudes. Consequently, the efficiency of the cross-modulation due to the nonlinearity of the contacts should decrease. This situation is illustrated in Fig. 7(b), for which the amplitude of the pump is the same as in Fig. 7(a), but the probe wave excitation is $\sim$30 dB higher (that is pump and probe amplitudes are comparable). As was argued above, the efficiency of the nonlinear perturbation of the contacts decreased noticeably for such strong probe-wave amplitude, so that the contrast in the modulation depth (for configurations with and without the insert in the saw-cut) is much smaller in Fig. 7(b) than in Fig. 7(a). This example

illustrates that, in nonlinear diagnostics, the sounding amplitudes should be chosen taking into account the amplitude scales of intrinsic nonlinearities of the defects. Thus the apparent straightforward choice 'the higher are the sounding amplitudes, the better are the observation conditions' is not always the best option in nonlinear methods.

In addition to previous control experiments with intact rod-shape samples, these experiments with the artificial defect have excluded doubts that the eventual parasite nonlinearities at the connections of the transducers to the sample could be important for the observed effects (since the comparison between damaged and reference samples in Section 3.1 inevitably implied either different transducers or different coupling of the same transducers for different samples). In contrast, in the discussed experiments with and without the insert in the saw-cuts, the state of all connections as well as the regimes of the electronics remained exactly the same. Therefore, such a method of creation of an artificial crack-like defect is rather useful for calibration purposes and for checking the importance of residual nonlinearities of all components of the setup. However, it should be clearly understood that the structure of the interfaces in such artificial crack-like defects in certain aspects differs essentially from the interface structure in real cracks. The main difference is associated with the fact that in real cracks their surfaces are initially matched and, due to the 2D-character of the material rupture, the contacts at their interface are predominantly of a strip-like (nearly cylindrical), rather than point-like shape. In contrast, in the artificial defect of the above described type, the contacting surfaces with micro-asperities are initially unmatched, so that the contacts are rather of point-like type than strip-like ones. Such point-like contacts may be quite numerous, so that their large amount may compensate their smaller efficiency from the point of view of the acoustic energy dissipation (and the influence on the elasticity) compared to the case of elongated contacts having much larger area. However, in certain aspects, the role of the local near-cylinder geometry of the contacts is not only quantitative, but results in important qualitative (functionally different) features. The respective effects will be considered in the Section 3.3. They provide an additional indication that the geometry of contacts in real cracks is predominantly quasi-cylindrical.

3.3. Slow dynamics due to temperature effects and super-slow modulation technique

Further studies of interaction of a stronger pump with a weaker probe wave revealed additional manifestations of inner contacts in cracks, which can be attractive for diagnostic applications. In particular, for samples containing individual cracks, pronounced logarithmic in time slow dynamics was found for parameters of resonance peaks of the probe wave [28]. The observed effects in certain features were similar to logarithmic in time slow relaxation reported in [29] for rock samples and attributed to slow restoration of large ensembles of some inner bonds, which were broken during the acoustic activation of the material. The mechanism of slow dynamics observed in our experiments should be essentially different than that discussed in [29], since the observed in our experiments slow drift of the resonance curve parameters was pronouncedly reversible and highly symmetrical for the acoustic activation and the subsequent relaxation. Besides, unlike rocks containing huge ensembles of defects we observed this reversible logarithmic slow dynamics for individual cracks. Namely, in glass samples, that were similar to those described in Section 3.1, we observed slow (on the scale 10^1–10^2 s) drifts of probe-wave resonances both during the acoustics activation of the sample by the pump excitation and in the subsequent relaxation after switching off the pump action [28].

Examples of the observed slow dynamics of the resonance frequency shifts and the complementary

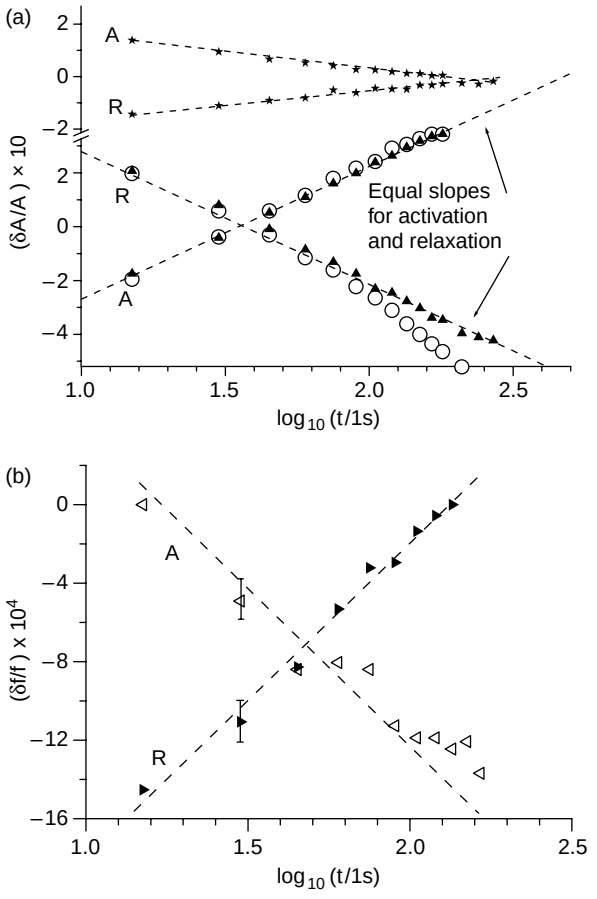

Fig. 8. Examples of the log-time dependence of the dissipation (a) and the resonance frequency shift (b) for different peaks in the glass rod with a crack. Letters A and R denote stages of activation of the sample and relaxation, for each stage time was counted from switching on and switching off the pump source, respectively. Slopes of the A-and R-lines exhibit pronounced symmetry. Triangles in figures (a) and (b) are for the same peak 3700 Hz, circles are for peak 3400 Hz and asterisks for peak 23, 700 Hz.

variations in the amplitude the resonance peaks (proportional to the variations in the quality factors) are shown in Fig. 8. In Fig. 8(b) the frequency shift is shown for one of the resonances (3700 Hz), the same as in Fig. 8(a). The pronounced symmetry (that is the same rate) of the observed parameter drift under the acoustics activation and during the subsequent relaxation is readily explained by the symmetry of the acoustically produced heating of inner contacts in cracks and their post-activation cooling. It is essential that the observed logarithmic character of the time dependences corroborates the earlier (see Section 3.1) independently drawn conclusion on the predominantly elongated near-cylinder shape of inner contacts in cracks. Indeed, the assumption of the nearly cylindrical contact geometry yields the following asymptotically-logarithmic expressions for the time-dependence of variations of local temperature $\tilde{T}$ of the inner contacts during the heating [28]:

$$\tilde{T} \approx \frac{Q_F(k=0)}{4\pi\rho CD} \ln\frac{t}{l^2/D}, \quad \text{at } t \gg l^2/D = \omega_l^{-1}. \tag{9}$$

Here ρ, C and $D=\kappa/(\rho C)$ are the material density, specific heat and thermal diffusivity; $Q_F(k)$ is the spatial Fourier transform of the source (due to acoustic production of heat at the contact in our case); l is the contact width. For the subsequent cooling (after switching off the source Q_F at time $t=t_0$) there is also a log-time approximate solution with the same factor before the logarithm:

$$\tilde{T} \approx \frac{Q_F(k=0)}{4\pi\rho CD} \left[\ln\frac{t_0}{l^2/D} - \ln\frac{(t-t_0)}{l^2/D}\right], \tag{10}$$

valid for $l^2/D \ll t-t_0 \leq t_0$. It is essential to note that the upper time-limit of the logarithmic behaviour (9) is determined by the time intervals $L^2/D \sim L^2/D$ during which the characteristic size of the heated region exceeds the scale $\tilde{L}$ of the contact length (which is comparable with the crack diameter L for elongated contacts). Upon reaching this threshold time, the heat propagation switches from quasi two-dimensional to three-dimensional regime. By this time, contact temperature practically reaches some saturated value, so that the temperature-induced acoustical manifestations (resonance frequency shift or quality-factor variations in the considered cases) do also reach saturation. For glass samples with cracks 3–4 mm in size the observed 100–150 s characteristic duration of the logarithmic behaviour agree well with the estimate $t_{char} \sim L^2/D$ [28] of the characteristic time scale in Eqs. (9) and (10). The understanding of the described features of the thermoelastic mechanism is important, since it opens a new possibility to evaluate the size of the defects via the observation of the mentioned above saturation of the log-time behaviour. Indeed, Eqs. (9) and (10) indicate that although the slope of the slow drifts depends on the intensity of acoustic thermal sources (which is practically impossible to estimate for unknown position of a defect even for a calibrated pump source), the characteristic saturation time does not depend on this unknown thermal-source intensity, but is determined by the size of the defect and by the thermal conductivity of the material, which is normally known. The considered mechanism thus predicts that the time-scale of the discussed slow-dynamics should be essentially different for materials with strongly different thermal conductivity, for example, for glass and steel. Such a quantitative difference corroborating the thermoelastic origin of the discussed effects has been really observed in additional experiments with steel samples containing a single crack.

In these experiments, in addition to brittle glass samples with cracks, qualitatively very similar slow dynamic effects have been found for acoustically activated steel test samples (about $36\times7\times6$ cm in size). The experimental arrangement was similar to that shown in Fig. 6. Each sample contained a single specially prepared subsurface crack with $\sim$10 mm characteristic size. In one sample the prepared crack was closed, in the other sample the crack was rather open and the third intact steel block served as a reference one. Examples shown in Fig. 9 are obtained for one of the probe wave resonances in the sample with the closed crack subjected to the acoustic activation at another pump frequency. Plots in Fig. 9(a) demonstrate a waterfall record

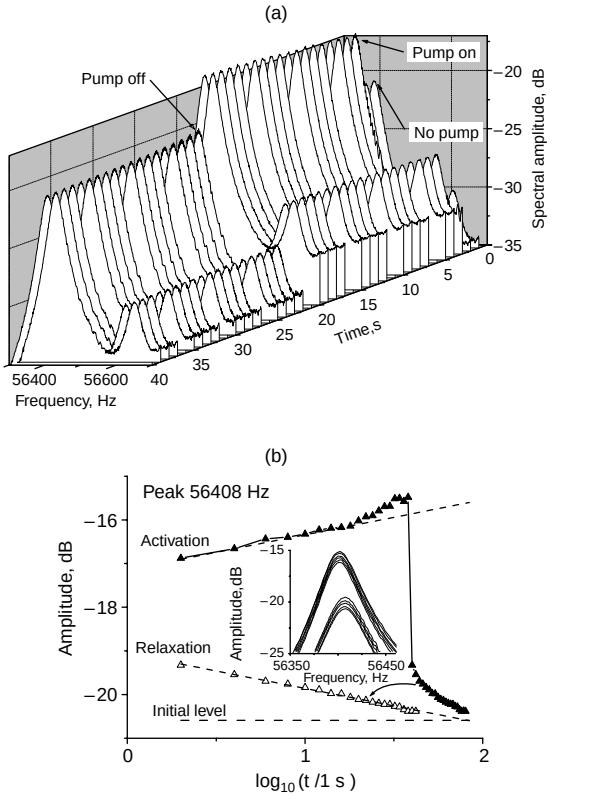

Fig. 9. Reversible slow dynamics with near-perfect symmetry between activation and relaxation for steel sample with closed crack. (a) Waterfall record for two probe peaks. (b) Temporal slice for peak 56,408 Hz; light triangles are for the relaxation plotted starting from the moment of switching off the pump. The inset shows overlapped probe-wave resonances for the stronger peak during activation and relaxation.

for two neighbouring resonance peaks with 2 s time interval between the successive records. Plot in Fig. 9(b) shows the time dependence of the amplitude for the peak around 56,400 Hz (compare to the upper plot in Fig. 8 for the glass sample). The overlapped resonance curves shown in the inset in Fig. 9(b) indicate that the resonance frequency is perturbed very weakly, which means that such a relatively small crack in the massive sample predominantly influences the quality factor (dissipation) much like for the glass sample (compare with the discussion of Fig. 5). Further, much like the plots in Fig. 8 the logarithmic of time dynamics of the resonance peak amplitudes in Fig. 9 exhibits pronounced symmetry between the activation (heating) and relaxation (cooling). As expected, in the steel sample the characteristic time scale of the near-logarithmic behaviour is smaller than that for the glass sample (about 35–45 s versus 100–150 in glass), which again correlates well with Eqs. (9) and (10) taking into account that the thermal conductivity is about 15 times higher for steel, whereas the crack (and likely the contact length) in steel is roughly twice larger than in the glass samples. These results on the dependence of the saturation time on the material parameters and crack's size confirm the possibility to quantify the defect scale using thermo-elastic slow dynamics.

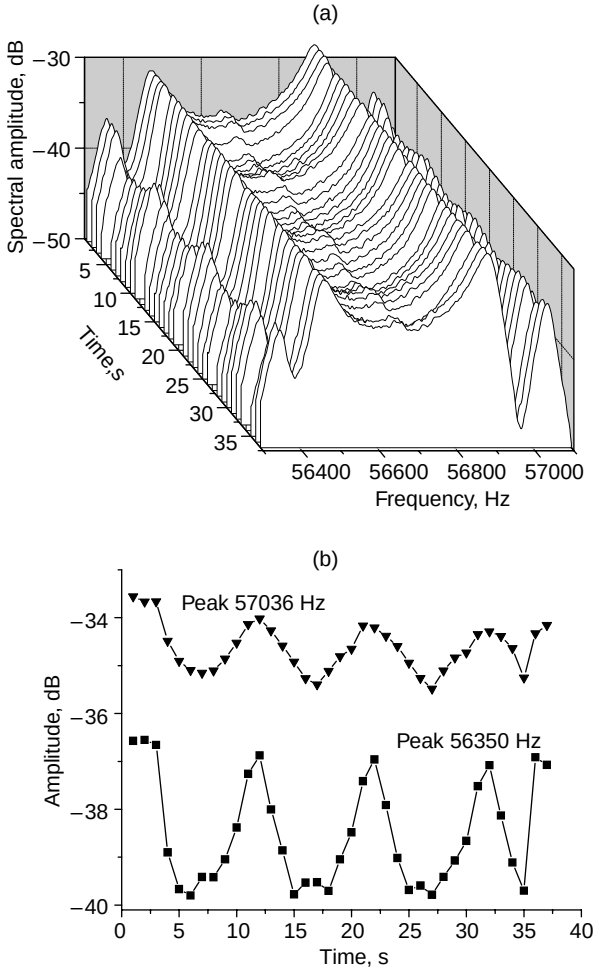

Fig. 10. Slow modulation of the probe-wave FRF by the pump action at 69 kHz and modulation frequency 0.1 Hz for the second sample with open crack. (a) Waterfall record for four probe wave peaks around 56 kHz indicating strong difference in the modulation depth. (b) Temporal slices for peaks at 56,350 and 57,036 Hz exhibit slow modulation with superimposed regular drift that is saturated by 30–35 s of activation.

Dependencies very similar to those shown in Fig. 9 (at the same time-scale) were obtained for the second sample that also contained a crack of a similar size. For that sample with loosely contacting crack interfaces the slow thermal effects (say on scales $\sim$10 s and more) were even stronger and were comparable with 'instantaneous' perturbations of the probe wave caused by the pump. This suggests an idea to combine the exploitation of the modulated pump action for obtaining the cross-modulation effect of the LG-type together with observations of slow drifts of the frequency-response function for the probe wave on the scale of tens of seconds. To this end the modulation frequency of the pump wave should be chosen low enough, for example, 0.1 Hz as shown in Fig. 10 for the records obtained for the second sample using such a slowly-modulated pump wave.

The waterfall plot in Fig. 10(a) demonstrates clearly that different resonances (even having rather close frequencies, but different spatial structures) are very differently affected by the crack, which opens a way to locate the crack position. Note also, that this difference between neighbour resonances confirms that the observed effects are definitely originated inside the sample and are not related to parasite nonlinearities in the electronics or at the contacts of the piezo-actuators with the sample. The temporal slices shown in Fig. 10(b) for two peaks (56,350 and 57,036 Hz) demonstrate very pronounced LG-type modulation with superimposed slow drift, the drift being saturated by 30–35 s of the activation as has been discussed above.

It is important to underscore that, for the reference intact steel block, the slow-dynamics effects have not been observed. The fast pump-induced variations in the probe wave resonance peaks (due to residual technical nonlinearities and the weak anharmonicity of the interatomic interaction in the sample bulk) did not exceed fractions of decibel versus typical 1–4 dB (or 10–60% variations) for the damaged samples shown in the examples in Figs. 9 and 10.

4. Conclusion

In the considered demonstrative experiments we used different samples containing either real cracks or artificial crack-like defects. The usage of transparent glass in some of the experiments facilitated direct visual estimation of the defect parameters. Comparison with the reference intact samples clearly indicated that the observed pronounced modulation was connected only with the presence of the defects.

Both the experimental data and the theoretical arguments corroborate that the new variant of the modulation technique is very sensitive to the presence of crack-like

defects and offers significant technical advantages (possibility to effectively use sample resonances both for the primary excitations and the modulation sidelobes; flexibility and independence in the choice of the working carrier and modulation frequencies; possibility to use compact piezo actuators even at arbitrary low modulation frequencies). The obtained results indicate that, in contrast to conventionally considered role of the elastic part of the sample nonlinearity, the effects of the amplitude-dependent dissipation may play the dominant role for the modulation effects in weakly damaged samples. This understanding is important for optimization of the parameters of the sounding pump and probe waves. Certainly, the considered thermoelastic modulation mechanism is not the unique one, so that the nonlinear-elastic or hysteretic mechanisms may be also important in other conditions.

Note, finally that in this communication we focused primarily on the physical features of the proposed cross-modulation and slow-dynamics approaches and pointed out main distinctions from the earlier discussed nonlinear acoustic (including modulation-type) methods of crack detection. For obtaining additional information on the defect localization the dependence of the cross-modulation and slow-dynamics effects on the particular spatial structure of the probe and pump waves may be used (see examples of this dependence in Section 3.2). The temporal scales of the slow drifts may be used for quantification of the defect size basing on the discussed above thermoelastic mechanism of the slow-dynamics effects. The new approach is rather flexible from the point of view of implementation, and it may be used either in the spectral cross-modulation form or in the form of the slow modulation of probe-wave resonances, or via direct comparison of the frequency-response functions in the absence and presence of the pump action including both fast and slow-dynamics effects.

Acknowledgements

The work was partially supported by RFBR (grant No 05-02-17355), Russian Science Support Foundation and DGA contract No. 00.34.026.00.470.75.65.

References

[1] Gitz ID, Guschin VV, Konyukhov BA. Measurements of nonlinear distortions of acoustic waves in polycrystalline aluminium in fatigue tests. Akust Zhurn (Sov Phys Acoust) 1973;19(3):335–8.
[2] Sessler JG, Weiss V. Patent US3867836, Crack detection apparatus and method; 1975.
[3] Buck O, Morris WL, Richardson JM. Acoustic harmonic generation at unbounded interfaces and fatigue cracks. Appl Phys Lett 1978;33(5):371–3.
[4] Antonets VA, Donskoy DM, Sutin AM. Nonlinear vibrodiagnostics of flaws in multilayered structures. Mech Compos Mater 1986;(5):934–7.
[5] Achenbach JD, Parikh OK, Sortiopoulus DA. Nonlinear effects in reflection from adhesive bonds. In: Thompson DO, Chimenti DE, editors. Review of progress in QNDE, vol. 8B, 1989. p. 1401–7.
[6] Rudenko OV. Nonlinear methods in acoustic diagnostics. Russ J Nondestr Test 1993;29(8):583–9.
[7] Korotkov AS, Sutin AM. Modulation of ultrasound by vibrations in metal constructions with cracks. Acoust Lett 1994;18:59–62.
[8] Ekimov AE, Didenkulov IN, Kazakov VV. Modulation of torsional waves in a rod with a crack. J Acoust Soc Am 1999;106(3):1289–92 [Pt. 1].
[9] Zaitsev VYu, Sas P. Nonlinear response of a weakly damaged metal sample: a dissipative mechanism of vibro-acoustic interaction. J Vib Control 2000;6:803–22.
[10] Van Den Abeele K, Johnson PA, Sutin AM. Nonlinear elastic wave spectroscopy (NEWS) techniques to discern material damage. Part I. Nonlinear wave modulation spectroscopy. Res Nondestr Eval 2000;12(1):17–30.
[11] Donskoy D, Sutin A, Ekimov A. Nonlinear acoustic interaction on contact interfaces and its use for nondestructive testing. NDT&E Int 2001;34:231–8.
[12] Kazakov VV, Sutin AM. Pulsed sounding of cracks with the use of the modulation of ultrasound by vibrations. Acoust Phys 2001;47(3):308–12.
[13] Kazakov VV, Sutin A, Johnson PA. Sensitive imaging of an elastic nonlinear wave-scattering source in a solid. Appl Phys Lett 2002;81(4):646–8.
[14] Kazakov VV, Johnson PA. Nonlinear wave modulation imaging. In: Rudenko OV, Sapozhnikov OA, editors. Nonlinear acoustics at the beginning of the 21st century, vol. 2. Moscow: Faculty of Physics, MSU; 2002. p. 763–6.
[15] Rokhlin SI, Wang L. Surface and interface characterization by nonlinear vibrations. In: Ibid., vol. 2. p. 775–8.
[16] Adler L, Rokhlin SI, Cantrell JH. Angle beam ultrasonic spectroscopy to evaluate adhesive layers: linear and nonlinear methods. In: Ibid., vol. 2. p. 747–50.
[17] Zaitsev V, Gusev V, Castagnede B. Observation of the 'Luxemburg—Gorky' effect for elastic waves. Ultrasonics 2002;40:627–31.
[18] Zaitsev V, Gusev V, Castagnede B. Luxemburg-Gorky effect retooled for elastic waves: a mechanism and experimental evidence. Phys Rev Lett 2002;89(10):105502 [1–4].
[19] Johnson PA, Guyer RA. The astonishing case of mesoscopic elastic nonlinearity. Phys Today 1999;(April):30–6.
[20] Van Den Abeele KEA, Sutin A, Carmeliet J, Johnson P. Micro-damage diagnostics using nonlinear wave spectrscopy (NEWS). NDT&E Int 2001;34:239–48.
[21] Landau LD, Lifschitz EM. Theory of elasticity. New York: Pergamon; 1986 [3rd (revised) english edition].
[22] Belyaeva IYu, Zaitsev VYu. Nonlinear elastic properties of microinhomogeneous hierarchically structured media. Acoust Phys 1997;43(5):594–9.
[23] Walsh JB. Seismic wave attenuation in rock due to friction. J Geophys Res 1966;71(10):2592–9.
[24] Gordon RB, Davis LA. Velocity and attenuation of seismic waves in imperfecty elastic rock. J Geophys Res 1968;73:3917–35.
[25] Mate CM, McClelland GM, Erlandsson R, Chiang S. Atomic-scale friction of a tungsten tip on a grafite surface. Phys Rev Lett 1987;59(17):1942–5.
[26] Mavko GM. Frictional attenuation: an inherent amplitude dependence. J Geophys Res 1979;84(B9):4769–75.
[27] Zaitsev VYu, Sas P. Dissipation in microinhomogeneous solids: inherent amplitude-dependent attenuation of a non-hysteretical and non-frictional type. Acust Acta Acust 2000;86:429–45.
[28] Zaitsev V, Gusev V, Castagnede B. Thermoelastic mechanism for logarithmic slow dynamics and memory in elastic wave interaction with individual cracks. Phys Rev Lett 2003;90(7):075501 [1–4].
[29] TenCate JN, Smith DE, Guyer R. Universal slow dynamics in granular solids. Phys Rev Lett 2000;85:1020–3.